Solid State Communications 299 (2019) 113649

Contents lists available at ScienceDirect

Solid State Communications

journal homepage: www.elsevier.com/locate/ssc

Communication

Location of oxygen vacancies in $Sr_2CuO_{3+\delta}$ single crystal determined by polarized EXAFS at Cu *K*-edge

H.B. Wang[a,b], W. Liang[c], Z.L. Luo[b], Q.Q. Liu[c], H.L. Huang[b], M.M. Yang[b], Y.J. Yang[b], S.X. Hu[b], Z. Jiang[e], S.D. Li[d], X. Sun[d], C.Q. Jin[c,*], C. Gao[b,d,f,**]

[a] Tonghua Normal University, Tonghua, Jilin 230026, China
[b] National Synchrotron Radiation Laboratory and School of Nuclear Science and Technology, University of Science and Technology of China, Hefei, Anhui 230026, China
[c] Institute of Physics, Chinese Academy of Sciences, Beijing 100080, China
[d] Department of Physics, University of Science and Technology of China, Hefei, Anhui 230026, China
[e] Shanghai Institute of Applied Physics, Chinese Academy of Sciences, Shanghai 201204, China
[f] CAS Key Laboratory of Materials for Energy Conversion and Collaborative Innovation Center of Chemistry for Energy Materials, University of Science and Technology of China, Hefei, Anhui 230026, China

ARTICLE INFO

Communicated by T. Kimura

Keywords:
$Sr_2CuO_{3+\delta}$ single crystal
Polarized EXAFS
Oxygen vacancy
High temperature cuprate superconductors

ABSTRACT

The location of oxygen vacancies in $Sr_2CuO_{3+\delta}$ single crystal has been studied by polarized extended x-ray absorption fine structure (PEXAFS) at Cu *K*-edge. We found that the oxygen vacancies locate both in the CuO_2 plane and at the apical site. Among the total 18 ± 8% oxygen vacancies, about 10 ± 5% locates in the CuO_2 plane and 8 ± 3% at the apical site.

1. Introduction

$Sr_{n+1}Cu_nO_{2n+1+\delta}$ series high temperature superconductors were first synthesized by Hiroi, Adachi and Han under high temperature and high pressure [1–3]. Among them, $Sr_2CuO_{3+\delta}$ (n = 1) shows a relatively high T_c of about 75 K. This temperature could be further increased to 95 K with an annealing in N_2 atmosphere, which is about twice of that of other doped 214-type cuprates [4–6]. Moreover, this compound exhibits a simple crystal structure: one CuO_2 plane sandwiched by two Sr_2O_2 rock salt layers. In such a structure, oxygen vacancy is the only carrier supplier of the CuO_2 plane. Due to this reason, the microstructure of $Sr_2CuO_{3+\delta}$ has been extensively studied. In these studies, a lot of effort was paid to the location and arrangement of the oxygen vacancies since the location and arrangement of the oxygen vacancies were found to be highly relevant to the high T_c superconducting mechanism [4,7]. For example, x-ray diffraction [7,8], neutron diffraction [9] and high resolution transmission electron microscopy [10–12] have demonstrated that the oxygen vacancies form superlattice and the symmetry of the superlattice changes from *C*2/*m* to *Cmmm* and *Pmmm* when the annealing temperature is increased to 150 °C and 250 °C [3,12,13]. However, there are a lot of studies showing contradictory results on the location of the oxygen vacancies. Hiroi and Liu believed that the oxygen vacancies locate at the apical site as in other high T_c superconductors [1,13]. Shimakawa and Wang claimed that the oxygen vacancies lay in the CuO_2 plane from Rietveld refinement of the neutron powder diffraction and transmission electron diffraction [9,10]. In 2007, F. J. Berry et al. [14] reported an EXAFS measurement on the $Sr_2CuO_{3+\delta}$ powder sample. By fitting the EXAFS oscillations with a two sub-coordination shell model, they suggested that the oxygen vacancies situate in the CuO_2 plane. Although these works help to understand the location of oxygen vacancies, they all are based on powder samples. The angular information of Cu–O coordination (in plane or apical direction) was also intrinsically lost in the measurement of powder samples. The in-plane and apical coordination information can not be distinguished around Cu atom. Therefore, the estimation of oxygen atoms coordination number around Cu was not exact. The capability of EXAFS to solve the different local bond lengths, while the diffraction gives only the average interatomic distance, was well demonstrated in solid solutions. In this paper, we report a polarized EXAFS study on the coordination of Cu in a superconducting

* Corresponding author.
** Corresponding author. National Synchrotron Radiation Laboratory and School of Nuclear Science and Technology, University of Science and Technology of China, Hefei, Anhui 230026, China.
E-mail addresses: jin@iphy.ac.cn (C.Q. Jin), cgao@ustc.edu.cn (C. Gao).

https://doi.org/10.1016/j.ssc.2019.113649
Received 11 April 2019; Received in revised form 27 May 2019; Accepted 31 May 2019
Available online 08 June 2019

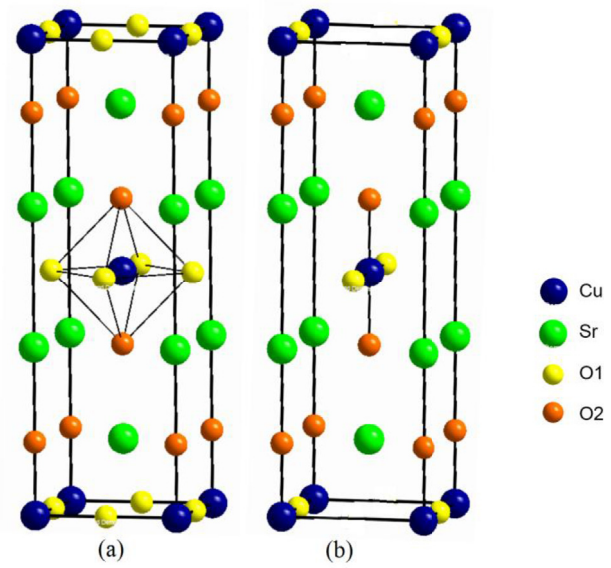

Fig. 1. Unit cells of (a) $Sr_2CuO_{3+\delta}$ and (b) Sr_2CuO_3 single crystals.

$Sr_2CuO_{3+\delta}$ single crystal. Using the angular resolution of linear polarization of synchrotron radiation x-ray, oxygen coordination of Cu, along and perpendicular to the CuO_2 plane, were directly measured. Through comparison with its parent compound Sr_2CuO_3 whose crystal structure is known, we found that oxygen vacancies in $Sr_2CuO_{3+\delta}$ occupy both apical and in-plane sites and the occupation probability was also estimated.

2. Experiment and calculation

$Sr_2CuO_{3+\delta}$ single crystal was synthesized at high temperature and high pressure. Details on the synthesis can be found in Ref. [15]. Shown in Fig. 1 are the unit cells of $Sr_2CuO_{3+\delta}$ and its parent compound Sr_2CuO_3. Fig. 2 presents the schematic diagram of polarized EXAFS measurement geometry, which was carried out in a fluorescence detection mode at beamline 14 W, Shanghai Synchrotron Radiation Facility. Horizontally polarized x-ray from the wiggler was incidence on the sample. *E* is the electric field of the incident x-ray, *a*, *b* and *c* are the crystallographic directions of the $Sr_2CuO_{3+\delta}$ single crystal, θ is the incident angle, respectively. $Sr_2CuO_{3+\delta}$ single crystal was cleaved along the (001) plane and its *b* axis was placed vertically so that angle

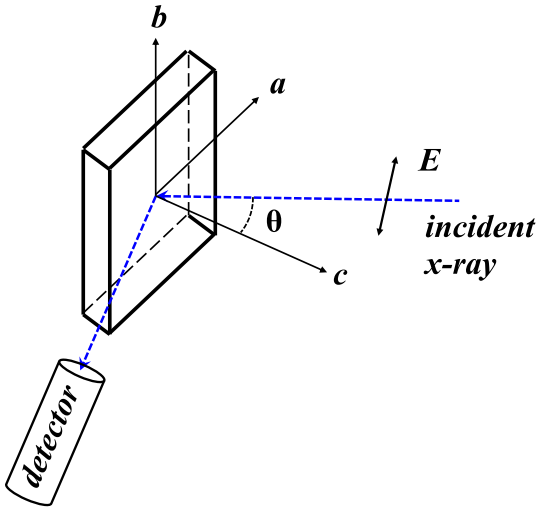

Fig. 2. Schematic diagram of the polarized EXAFS measurement geometry.

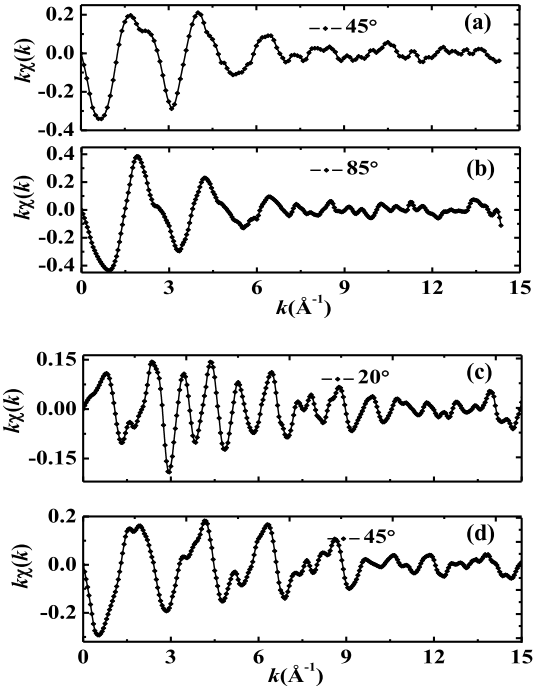

Fig. 3. (a) and (b) are the normalized EXAFS oscillations of $Sr_2CuO_{3+\delta}$ at incident angle of θ = 45° and θ = 85°. (c) and (d) are the normalized EXAFS oscillations of Sr_2CuO_3 at incident angle of θ = 20° and θ = 45°, respectively.

between *E* and *c* complements the incident angle. Fluorescent detector was placed horizontally and perpendicular to the incident x-ray. By rotating the sample around the *b* axis, polarized EXAFS at different incident angles were collected.

Based on density functional theory (DFT), the VASP software package with plane wave as the basic vector is used in the calculation. The electron exchange correlation potential is described by the generalized gradient function in the form of PBE. The electron-ion interaction is described by projection affix plus plane wave, and the cut-off energy of plane wave is set to 400 eV.

3. Results and discussion

Shown in Fig. 3(a) and (b) are the normalized Cu *K*-edge EXAFS oscillations of $Sr_2CuO_{3+\delta}$ single crystal at incident angle of 85° and 45°. For comparison, normalized Cu *K*-edge EXAFS oscillations of Sr_2CuO_3 single crystal at incident angle of 20° and 45° are shown together in Fig. 3(c) and (d). According to Stern and Lee [16–18], the polarized EXAFS oscillations of a single crystal can be expressed as:

$$\chi(k,\theta) = \frac{m\pi}{h^2}\sum_i 3\cos^2\theta_i N_i \frac{S_0^2}{kR_i^2} f_i(k,R_i) e^{-2R_i/\lambda} e^{-2k^2\sigma_i^2} \sin[2kR_i + \delta_i(k)], \quad (1)$$

where m, h, k, λ and S_0^2 are the electron mass, Planck constant, wave vector of the photoelectron, electron mean free path and amplitude loss factor, respectively. θ_i, N_i, R_i, f_i, σ_i^2 and δ_i are the angle of the coordination atom with respect to the electric field of the polarized synchrotron radiation x-ray, coordination number, coordination distance, scattering amplitude, mean square average displacement (Debye-Waller factor) and phase shift of the *i*th neighboring atoms, respectively. Substituting in the coordination values of the in-plane and apical oxygen, polarized EXAFS oscillations of $Sr_2CuO_{3+\delta}$ for $E\|a$ (χ_a) and $E\|c$ (χ_c) can be extracted from the measured EXAFS oscillations at incident angles of 85° (χ_{85}) and 45° (χ_{45}):

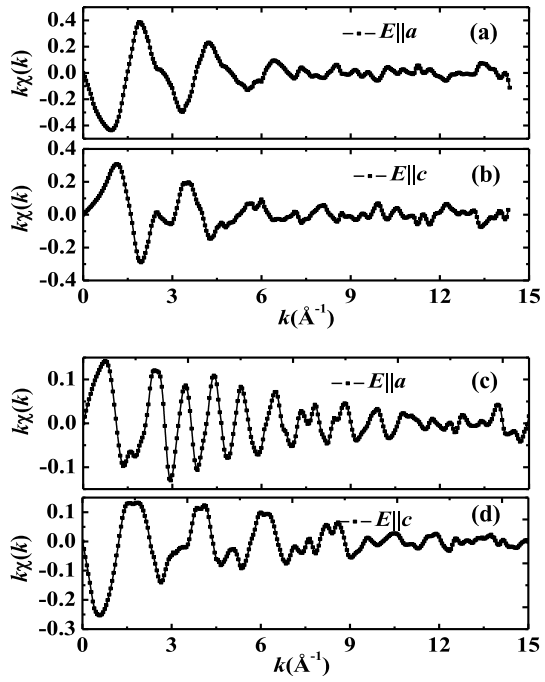

Fig. 4. (a) and (b) are the normalized EXAFS oscillations of $Sr_2CuO_{3+\delta}$ with $E\|a$ and $E\|c$. (c) and (d) are the normalized EXAFS oscillations of Sr_2CuO_3 with $E\|a$ and $E\|c$.

$$\chi_a = \frac{2\sin^2 85°\chi_{45} - \chi_{85}}{3(\sin^2 85° - \cos^2 85°)}$$
$$\chi_c = \frac{\chi_{85} - 2\cos^2 85°\chi_{45}}{3(\sin^2 85° - \cos^2 85°)}, \quad (2)$$

which were shown in Fig. 4(a) and (b). $E\|a$ detects the in-plane coordination while $E\|c$ detects the out-of-plane coordination. For comparison, shown in Fig. 4(c) and (d) are the oscillations of Sr_2CuO_3. Shown in Fig. 5 are the Radial-Structure-Functions (Fourier transform of the EXAFS oscillations) of Cu coordination along *a* and *c* directions in $Sr_2CuO_{3+\delta}$ and Sr_2CuO_3. The first strong peak is the Cu–O coordination. Obviously, there is significant anisotropy between the in-plane and out-of-plane Cu–O coordination. In order to get detailed coordination information, the Cu–O coordination peak was filtered out with a Hanning window and *k*-weighted inversely Fourier transformed to the *k* space. Considering the difference between the oxygen vacancies in the CuO_2 plane and at apical site, a two sub-coordination shell model was used to fit the polarized EXAFS oscillations of $Sr_2CuO_{3+\delta}$, as in Ref. [19]. As there is no oxygen vacancy in Sr_2CuO_3, single shell model was used to fit the polarized EXAFS oscillations of Sr_2CuO_3. The best fitting results are plotted in Fig. 6 and the best fitting parameters are listed in Table 1, for both $Sr_2CuO_{3+\delta}$ and Sr_2CuO_3. For Sr_2CuO_3, we found that Cu–O bond lengths along *a* and *c* directions are 1.957 Å and 1.962 Å, and the corresponding coordination numbers are 2.0 ± 0.2 and 2.0 ± 0.1, respectively. These parameters are well consistent with the crystallographic data of Sr_2CuO_3 [20], indicating the good reliability of this method. For $Sr_2CuO_{3+\delta}$, we found that there are two different Cu–O bonds for both in-plane and out-of-plane Cu–O coordination. The in-plane coordination consists of two Cu–O bonds with lengths of 1.848 Å and 1.889 Å, and the corresponding coordination numbers are 0.6 ± 0.2 and 1.0 ± 0.1, respectively. The out-of-plane coordination consists of two Cu–O bonds with lengths of 1.877 Å and 2.000 Å, and the corresponding coordination numbers are 1.0 ± 0.1 and 0.7 ± 0.1, respectively. These results indicate that the oxygen vacancies exist both in the CuO_2 plane and at the apical site. The total amount of oxygen vacancies is estimated to be about [(0.3 ± 0.1)+(0.4 ± 0.2)]/4 = 18 ± 8%. Here, the tetragonal symmetry of $Sr_2CuO_{3+\delta}$ single crystal is considered. Among the oxygen vacancies, about (0.3 ± 0.1)/4 = 8 ± 3 locates at the apical site and (0.4 ± 0.2)/4 = 10 ± 5% in the CuO_2 plane. In this way, δ in $Sr_2CuO_{3+\delta}$ is estimated to be about 0.3 ± 0.5, which is lower than the optimal doping of 0.4. This is consistent with its low T_c (about 35 K) as compared with the optimum critical temperature (75 K) [13].

According to the crystal field theory [21], oxygen vacancies in the CuO_2 plane will weaken the electrostatic repulsive interaction between O 2p and Cu 3d outermost orbital electrons and shorten the in-plane Cu–O coordination length. Similarly, oxygen vacancies at the apical site will weaken the bonding between Sr and O in the rock salt layer and

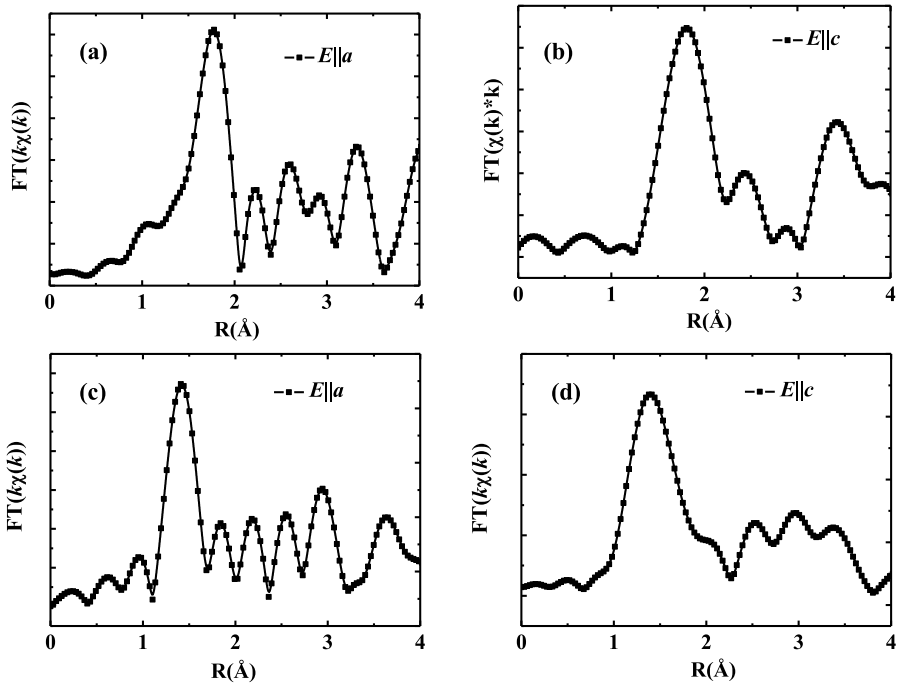

Fig. 5. (a) and (b) are the Radial-Structure-Functions (Fourier transform of the EXAFS oscillations) of $Sr_2CuO_{3+\delta}$ with $E\|a$ and $E\|c$. (c) and (d) are the Radial-Structure-Functions of Sr_2CuO_3 with $E\|a$ and $E\|c$.

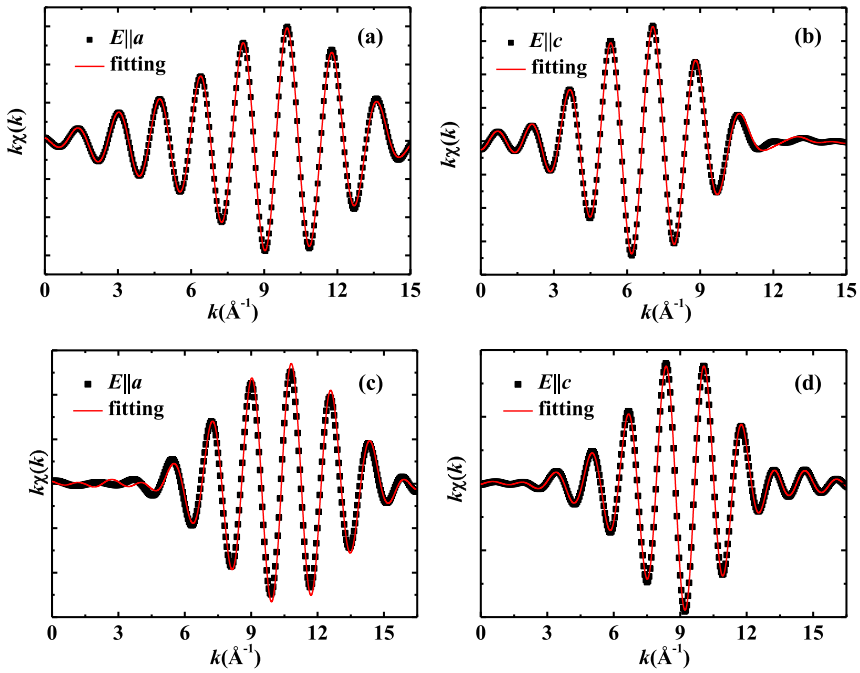

Fig. 6. (a) and (b) are the Fourier-filtered EXAFS oscillations (k-weighted inverse Fourier transform of the first strong peak) of the Cu–O coordination in $Sr_2CuO_{3+\delta}$ with $E\|a$ and $E\|c$. (c) and (d) are the EXAFS oscillations of Cu–O coordination in Sr_2CuO_3 with $E\|a$ and $E\|c$.

Table 1
Best fitting parameters for the Cu–O EXAFS oscillations in $Sr_2CuO_{3+\delta}$ and Sr_2CuO_3 single crystals.

		R(Å)	N
$Sr_2CuO_{3+\delta}$	$E\|a$	1.848	0.6 ± 0.2
		1.889	1.0 ± 0.1
	$E\|c$	1.877	1.0 ± 0.1
		2.000	0.7 ± 0.1
Sr_2CuO_3	$E\|a$	1.957	2.0 ± 0.2
	$E\|c$	1.962	2.0 ± 0.1

stretch the out-of-plane Cu–O coordination. Therefore, the longer in-plane Cu–O bond (bond length: 1.889 Å, coordination number: 1.0 ± 0.1) and shorter out-of-plane Cu–O bond (bond length: 1.877 Å, coordination number: 1.0 ± 0.1) belong to the undisturbed CuO_6 octahedral coordination, while the shorter in-plane Cu–O bond (bond length: 1.848 Å, coordination number: 0.6 ± 0.2) and longer out-of-plane Cu–O bond (bond length: 2.000 Å, coordination number: 0.7 ± 0.1) belong to the defect CuO_6 octahedral coordination with an oxygen vacancy situation on the CuO_2 plane or at the apical site, respectively.

In order to confirm the above experimental results, the VASP software package with plane wave as the basic vector is used in the calculation. Because of the large cell size ($2\sqrt{2}a_p \times 2\sqrt{2}a_p \times c_p$), only one K point, Gama point, is used in Brillouin region. Only one of the four CuO_6 octahedrons shown in Fig. 7 is included in such a large cell. This model mainly considers the effect of a single oxygen vacancy on the local structure. Firstly, the structure is optimized. All atoms in the cell can relax freely until the force acting on each atom is less than 0.01 eV/Å. At this time, the model is considered as a stable structure model. By analyzing the coordination situation, it is found that the coordination bond lengths of these four models are as shown in Table 2. The calculated Cu–O coordination bond lengths are in good agreement with the experimental results. Therefore, it can be judged that the crystal structure of $Sr_2CuO_{3+\delta}$ material is complex, resulting in a variety of superlattice structures.

According to the above analysis, the unusual Cu–O coordination of $Sr_2CuO_{3+\delta}$ may due to various reasons. The experimental results for Cu–O (in-plane) and Cu–O (apical) were the average result for each direction. Multi shell (more than two) for $Sr_2CuO_{3+\delta}$ may provide the similar bond length with Sr_2CuO_3. The modulated structures for $Sr_2CuO_{3+\delta}$ were complicated. The Jahn-Teller effect may not be the main factor affecting the local structure around Cu atom of $Sr_2CuO_{3+\delta}$. Therefore, the variation of bond length of Cu–O coordination is

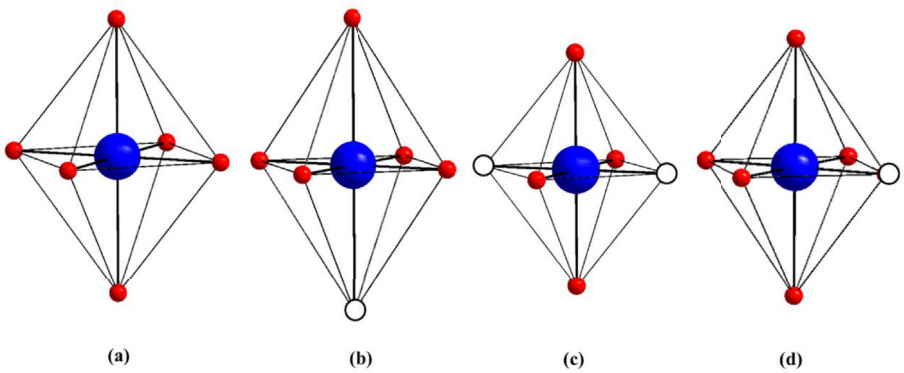

Fig. 7. (a) Intact CuO_6 octahedron; (b) CuO_6 octahedron with apical O_h; (c) CuO_6 octahedron with diagonal distribution of two O_hs in-plane; (d) CuO_6 octahedron with one O_h in-plane.

Table 2
In-plane and out-of-plane coordination bond lengths of CuO_6 octahedron shown in Fig. 7

CuO_6 octahedron	In-plane coordination bond lengths of Cu–O (Å)	out-of-plane coordination bond lengths of Cu–O (Å)
Intact CuO_6 octahedron	1.919	1.942
CuO_6 octahedron with apical O_h	1.876	1.962
CuO_6 octahedron with diagonal distribution of two O_hs in-plane	1.846	1.877
CuO_6 octahedron with one O_h in- plane	1.862	1.885

unusual.

The presence of oxygen vacancies in the CuO_2 plane may be compatible with, through phase separation, the generally believed viewpoint that perfect CuO_2 plane is essential for the superconductivity. As reported in refs. 12 and 13, Sr2CuO3 + δ consists of several modulated phases. Among them, at least *Fmmm*, which was believed to be non-superconducting, shows in-plane oxygen vacancy occupation. So, Sr2CuO3 + δ is a mixture of superconducting and non-superconducting phases. Our PEXAFS results support this opinion. The less apical oxygen vacancy ratio coincides with the small superconducting volume fraction [15]. To address these in-depth questions, further comprehensive microstructure characterization is needed.

4. Conclusions

In conclusion, the location of oxygen vacancies in high temperature superconductor $Sr_2CuO_{3+\delta}$ single crystal was studied by polarized EXAFS. The results show that the oxygen vacancies locate both in the CuO_2 plane and at the apical site with the ratio of about 10 ± 5% and 8 ± 3%, respectively.

Acknowledgments

This work was supported by the National Basic Research Program of China (2012CB922004, 2010CB934501, 2012CB933702),Science and technology topics of Jilin Provincial Department Education, China in 13th Five-Year (JJKH20180860KJ) and the Natural Science Foundation of China. The authors appreciate the beam time provided from beam line BL14W of SSRF.

References

[1] Z. Hiroi, M. Takano, M. Azuma, Y. Takeda, Nature 364 (1993) 315.
[2] S. Adachi, H. Yamauchi, S. Tanaka, N. Môri, Physica C 212 (1993) 164.
[3] P.D. Han, L. Chang, D.A. Payne, Physica C 228 (1994) 129.
[4] H. Yang, Q.Q. Liu, F.Y. Li, C.Q. Lin, R.C. Yu, Supercond. Sci. Technol. 20 (2007) 904.
[5] J.M. Tarascon, L.H. Greene, W.R. Mckinnon, G.W. Hull, T.H. Geballe, Science 235 (1987) 4794.
[6] J.H. Wen, Z.J. Xu, G.Y. Xu, J.M. Tranquada, G. Gu, S. Chang, H.J. Kang, Phys. Rev. B 78 (2008) 212506.
[7] Q.Q. Liu, X.M. Qin, Y. Yu, F.Y. Li, C. Dong, C.Q. Jin, Physica C 420 (2005) 23.
[8] P. Laffez, X.J. Wu, S. Adachi, H. Yamauchi, N. Mori, Physica C 222 (1994) 303.
[9] Y. Shimakawa, J.D. Jorgensen, J.F. Mitchell, B.A. Hunter, H. Shaked, D.G. Hinks, R.L. Hitterman, Z. Hiroi, M. Takano, Physica C 228 (1994) 73.
[10] Y.Y. Wang, H. Zhang, W.P. Dravid, L.D. Marks, P.D. Han, D.A. Payne, Physica C 255 (1995) 247.
[11] H. Zhang, Y.Y. Wang, L.D. Marks, W.P. Dravid, P.D. Han, D.A. Payne, Physica C 255 (1995) 257.
[12] Q.Q. Liu, H. Yang, X.M. Qin, L.X. Yang, F.Y. Li, Y. Yu, R.C. Yu, C.Q. Jin, S. Uchida, Phys. C Supercond. 460 (2007) 56.
[13] Q.Q. Liu, H. Yang, X.M. Qin, Y. Yu, L.X. Yang, F.Y. Li, R.C. Yu, C.Q. Jin, S. Uchida, Phys. Rev. B 74 (2006) 100506.
[14] R.J. Berry, C. Greaves, R.C. Lobo, Polyhedron 11 (1992) 2331.
[15] W. Liang, Q.Q. Liu, L. Liu, T. Kakeshita, S. Uchida, C.Q. Jin, Sci. China Phys. Mech. Astron. 56 (2013) 1.
[16] E.A. Stern, Phys. Rev. B 10 (1974) 3027.
[17] E.A. Stern, S.M. Heald, Handbook on Synchrotron Radiation vol. 1, (1983), p. 955.
[18] P.A. Lee, P.H. Citrin, P. Eisenberger, B.M. Kincaid, Rev. Mod. Phys. 53 (1981) 769.
[19] A. Bianconi, N.L. Saini, A. Lanzara, M. Missori, T. Rossetti, H. Oyanagi, H. Yamaguchi, K. Oka, T. Ito, Phys. Rev. Lett. 76 (1996) 3412.
[20] I.B. Bobylev, S.V. Naumov, N.A. Zyuzeva, Phys. Solid State 55 (2013) 1602.
[21] R.G. Burns, W.S. Fyfe, Researches in Geochemistry vol. 2, (1967), p. 259.